*Korean J. Chem. Eng.*, 40(10), 2434-2441 (2023)
DOI: 10.1007/s11814-023-1447-6

pISSN: 0256-1115
eISSN: 1975-7220

# Thioanisole oxidation promoted by new niobium-based catalyst: The effect of surface hydroxyl groups on catalytic performance

**Guilherme Carletti de Aguiar*, Daniel Carreira Batalha*, Humberto Vieira Fajardo*, José Balena Gabriel Filho**, Carlos Giovanni Oliveira Bruziquesi**, Luiz Carlos Alves de Oliveira**, Mateus Aquino Gonçalves***, Teodorico de Castro Ramalho***, and Adilson Candido Silva*,†**

*Department of Chemistry, Federal University of Ouro Preto, 35400-000, Ouro Preto, MG, Brazil
**Department of Chemistry, Federal University of Minas Gerais, 31270-901, Belo Horizonte, MG, Brazil
***Department of Chemistry, Federal University of Lavras, 37200-000, Lavras, MG, Brazil
(*Received 11 October 2022 • Revised 6 January 2023 • Accepted 31 January 2023*)

**Abstract**−In this work, the application of a new, synthesized niobium-based catalyst, called S4 (niobium oxyhydroxide), in the liquid-phase oxidation of methyl-phenyl sulfide (thioanisole) using hydrogen peroxide as oxidant was proposed. The synthetic method employed provided a material with low crystallinity and high specific surface area and acidity. A commercial material, called HY-340 (hydrated niobium oxide), was also employed as heterogeneous catalyst for comparative purposes. The results showed that the synthesized S4 material is an outstanding catalyst, being able to completely convert the substrate (thioanisole) that achieves almost 90% of selectivity for methyl phenyl sulfone formation, under mild reaction conditions. According to the theoretical and experimental combined results, the superior performance of S4 catalyst is related to the better interaction of $H_2O_2$ and thioanisole molecules with S4 surface, compared to HY-340, pointing to the greater ability of this catalyst to form reactive oxygen species in contact with hydrogen peroxide, due to its higher content of free hydroxyl groups present on its surface.

Keywords: Niobium, Thioanisole, Oxidation, Heterogeneous Catalysis

## INTRODUCTION

Due to the great potential that Brazil has regarding its niobium resources, many studies have been carried out by Brazilian research groups from different areas of science and technology in the hope of finding new applications for this element. Brazil holds approximately 98% of the world's niobium reserves, accounting for about 97% of world production [1,2]. Due to the peculiar physical and chemical properties, niobium-based compounds have a wide range of applications, including heterogeneous catalysis. The main characteristics that make them promising candidates for use in a huge range of catalytic processes are their physicochemical stability, acidic and redox properties and versatility. In this way, these compounds can act as promoter or active phase, support, solid acid catalyst or redox materials [3-7]. In terms of acidity, niobium-based catalysts, such as niobium oxide ($Nb_2O_5$) and niobium oxyhydroxide ($NbO_2OH$), have important Lewis and Brønsted acid sites, which potentially act in many oxidation reactions through interactions with hydrogen peroxide ($H_2O_2$) molecules, in which surface oxidizing groups can be generated. In general, the use of hydrogen peroxide, both as an oxidizing agent and in a pre-treatment step, aims to form a highly reactive system capable of boosting various catalytic oxidation reactions. Depending on the nature of the catalyst surface, several types of reactive oxygen species ($OH^-$, $\cdot OH$, $O_2^-$, $O_2^{2-}$) can be generated in contact with $H_2O_2$. The formation of these species improves the oxidative properties of niobium-based catalysts, since the active oxygen species formed will promote oxidation of different substrates [8-14].

In the set of oxidative processes, the oxidation of sulfides to sulfoxides and sulfones has been extensively studied due to the importance of these products as building blocks in organic synthesis that are also utilized by the pharmaceutical and agrochemical industries. Due to stricter regulations to restrict the sulfur content of fuel oils intending to reduce the health and environmental dangers, this process is also very important for the petrochemical industry in the production of low sulfur fuels through oxidative desulfurization [15-19]. Currently, many metal-based catalysts have been studied for sulfide oxidation reactions, in the presence of a suitable oxidizer. However, the process commonly requires a long reaction time, at high temperatures and prolonged treatment using toxic materials, such as homogeneous heavy metal salts [20-29]. To circumvent the problems related to the use of toxic and non-green reagents, it is important to adapt the reaction parameters. Some of these modifications can be considered, for example by application of a heterogeneous catalyst, which is easily recoverable, causes low waste generation, and also can perform the reaction at lower temperatures, as well as the conjugated utilization of hydrogen peroxide, an efficient oxidant with easy handle, cheap and generates only water as by-product, therefore considered an attractive green oxidant [29-31]. There are notable works in the literature exploring the application of niobium based heterogeneous catalysts in the methyl phenyl sulfide (thioanisole) oxidation using $H_2O_2$ that include activated

†To whom correspondence should be addressed.
E-mail: adilsonqui@ufop.br

carbon supported amorphous $Nb_2O_5$ and mesoporous niobosilicates catalysts [29,32]. However, based on the scarce number of papers using niobium oxyhydroxide in the thioanisole oxidation, a comparative study was proposed between synthesized niobium oxyhydroxide (S4) and a commercial niobium oxide (HY-340) for the thioanisole oxidation at room temperature with hydrogen peroxide as oxidant. The physical and chemical properties of niobium-based compounds, including the acidity, depend on their structure. S4 sample was synthesized by a new and simple method developed by our group, which led to obtaining a catalyst with high specific surface area and high surface acidity. This work is, as far as we know, the first of its kind concerning the synthesis of niobium oxyhydroxide and its application as heterogeneous catalyst towards the oxidation of thioanisole. This study has revealed important theoretical and experimental results concerning the interaction between the surface of the catalysts and $H_2O_2$ as well as thioanisole and its consequences on their performance in the proposed reaction. It was possible to reach 100% of thioanisole conversion and high selectivity toward sulfone applying S4 synthesized catalyst. The surface properties presented by these materials, such as acidity, have directly influenced the catalytic reaction results, which were theoretically demonstrated by single point calculations.

## EXPERIMENTAL

### 1. Chemicals

1-Butanol (99%), 1-Hexanol (99%) and cetyltrimethylammonium bromide (CTAB, 99%) were purchased from Vetec (Brazil). Thioanisole (≥99%), Methyl phenyl sulfoxide (≥97%) and Methyl phenyl sulfone (≥98%) were purchased from Sigma-Aldrich. $NH_4OH$ (28 wt% $NH_3$ in water) was purchased from Qhemis (Brazil). Ultrapure water (Mili-Q Water) was used only in the synthesis (Gehaka, model MS2000). For the catalytic reactions, distilled water was used. Commercial niobic acid was kindly provided by the Companhia Brasileira de Metalurgia e Mineração (Araxá, Minas Gerais, Brazil).

### 2. Catalyst Preparation

The niobium oxyhydroxide synthesis (S4) was carried out according to a modification of the procedure previously described by Gabriel and co-workers [33]. S4 sample was initially prepared by adding 14 g of $NbCl_5$ to a system composed of 1-Butanol, 1-Hexanol, Mili-Q water and CTAB Surfactant under stirring at 60 °C and precipitated with $NH_4OH$ until reaching pH 7.5. After 6 hours of stirring at 75 °C, phase separation was observed, the lower one being colorless and the upper one being white. The upper phase was transferred to another recipient to be washed with Milli-Q water and then centrifuged. Finally, it was dried in an oven at 80 °C for 48 hours. Commercial hydrated niobium oxide (HY-340) was kindly provided by CBMM (Brazilian Metallurgy and Mining Company).

### 3. Catalyst Characterization

The structures of the catalysts were characterized by X-ray diffraction (XRD) at room temperature, from 10 to 60° $2\theta$, and a step of 0.02°, with an angular speed of 2°·min$^{-1}$ as Cu K$\alpha$ ($\lambda$=1.542 Å) radiation (Siemens model D-5000).

$N_2$ adsorption/desorption isotherms were obtained at 77 K by an automatic adsorption instrument (Autosorb IQ2 Quantachrome Instruments) to calculate the specific surface area and pore size distribution parameters according to the Brunauer-Emmett-Teller (BET) and Barrett-Joyner-Halenda (BJH) methods, respectively. Previously, the samples were degassed at 200 °C under nitrogen flow for 12 hours.

The acidity of the catalysts was determined by the pyridine adsorption method. Prior to analysis, 10 mg of each solid was weighed in small cups, which were placed in a quartz tube inside a tubular oven under constant $N_2$ flow at 120°C for 2 hours. The next step was the chemisorption of pyridine, where the acid sites were saturated by the probe molecule in the oven was kept at 50 °C, under a continuous flow for 2 hours. After adsorption, the oven temperature was raised to 120 °C, under the $N_2$ flow, for 1 hour for the removal of the eventual physisorbed pyridine. For the acquisition of spectral data, tablets were made of the materials with pyridine adsorbed on acidic sites by the Digilab Excalibur, series FTS 3000 infrared spectrometer. These discs were made by mixing 10 mg of the materials with 80 mg of KBr, pressing under vacuum at 6 t·cm$^{-2}$ for 3 minutes. The spectra were recorded in range of 1,700-1,400 cm$^{-1}$, with a resolution of 2 cm$^{-1}$ and 64 scans.

The number of acid sites of the catalysts was determined by the titration method. For the measurements, 20 mL of a NaOH aqueous solution (0.01 mol·L$^{-1}$) were added to the catalyst (10 mg). The mixture was kept under stirring for 24 hours, at room temperature. The supernatant solution was then separated by centrifugation and titrated with HCl aqueous solution (0.05 mol·L$^{-1}$) using phenolphthalein as indicator. Then, the quantity of acid sites ($H^+$/g) in the catalysts was determined by the equation: number of acid sites=[[initial quantity of NaOH added (moles)−quantity of HCl consumed (moles)]×Avogadro constant]/catalyst mass (g).

### 4. Catalytic Performance Test

Liquid-phase catalytic oxidation of thioanisole reactions were carried out in a one-necked round-bottom with a magnetic stir bar. The reaction conditions were the following: 2.5-10 mg of catalyst; 25, 40 and 60 °C of reaction temperature; 4.80-4.95 mL of solvent (chloroform - Synth, acetonitrile - Synth and methanol - Synth), 0.1 mL of thioanisole (Sigma-Aldrich) and 0.05-0.2 mL of hydrogen peroxide (Synth $H_2O_2$, 29% v/v). A kinetic study was performed from 15 minutes until 3 hours of reaction. Upon completion, the catalytic reaction was quenched. Finally, the solid catalyst and liquid phase were separated by centrifugation for five minutes at 3,000 rpm. For the conversion and selectivity acquisition data, an aliquot of the reaction medium was previously diluted in acetonitrile and injected into the gas chromatograph (Agilent GCFID-789B) equipped with a capillary column (HP-Innowax). Thioanisole conversion and selectivity for each product were quantified with the help of calibration curves, which were obtained by injecting each authentic product of known concentrations, using n-dodecane (Exodo, 99%) as the internal standard. To obtain the calibration curves for gas chromatographic analyses, five concentration levels (10-400 ppm) of the respective analyte were prepared from successive dilutions of a standard stock solution obtained from the reference substance. For the standard stock solution preparation, an appropriate quantity of each analyte was weighed out (taking into account the percent purity) and brought to volume in a 5.0 mL volumetric flask with the acetonitrile. Conversion and selectivity were calculated by: Conversion (%)=(moles of reactant reacted/initial moles of reac-

tant used)×100; Selectivity (%)=(total moles of product formed/moles of reactant reacted)×100.

**5. Computational Methods**

For computational methods, initially, the structures were built using the Gauss View 5.0 program, optimization, and single point calculations were performed using the Gaussian 09 software [34] with the B3LYP functional and the base set 6-31 g for all atoms.

## RESULTS AND DISCUSSION

**1. Characterization**

Fig. 1 shows the XRD patterns for S4 and HY-340 samples. The XRD diffractograms present non-crystalline material profiles. For S4 sample, the diffraction peaks present low intensity and are broader, indicating that this sample has lower crystallinity than HY-340. This can be due to the absence of thermal treatment during S4 synthesis. Fig. 2 displays the $N_2$ adsorption-desorption isotherms and pore diameter distributions of the S4 and HY-340. Both samples show type IV isotherms with hysteresis loops, typical of mesoporous materials. This characteristic is commonly found in amorphous niobium compounds [35,36]. In particular, the hysteresis is H4-type, which is composed of types I and II, more pronounced uptake at lower relative pressures and commonly associated with the filling of micropores [37]. Mesoporous isotherm profiles show hysteresis and can be related to the pore structure of the material. According to the IUPAC classification of hysteresis loops, the HY-340 has an H4-type, linked to pore with similar geometry, and the S4 catalyst presents an H2(b)-type profile, due to the pore-blocking effect inside the neck, generally bottle-type pores. Specific surface areas of 198 $m^2 \cdot g^{-1}$ and 169 $m^2 \cdot g^{-1}$ and pore volumes of 0.310 $cm^3 \cdot g^{-1}$ and 0.180 $cm^3 \cdot g^{-1}$ were measured for S4 and HY-340, respectively (Table 1). In addition to the use of the surfactant be able to influence the morphology of the solid, such as nucleation and growth of the particles during the synthesis, it also allowed differences in the specific surface area and pore volume values of the resulting material (S4), in relation to the HY-340 material, leading to, in this case, an increase in these values [35,36,38-40]. This result indicates that the method of synthesis used provided the material with larger specific surface area and porosity comparatively to the commercial HY-340. Infrared spectroscopy with adsorbed pyridine was used to identify the nature and amount of acidic sites (Brønsted and Lewis) on the surface of the catalysts. The infrared spectrum (Fig. 3) for the synthesized S4 showed bands at 1,442 $cm^{-1}$, characteristic of the Lewis acid site (Py-L), at 1,486 $cm^{-1}$, charac-

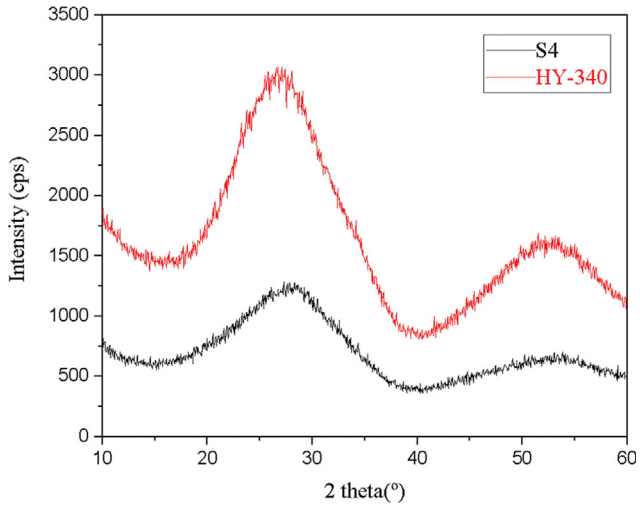


**Fig. 1. XRD patterns of S4 and niobium oxide (HY-340) without previous thermal treatment.**

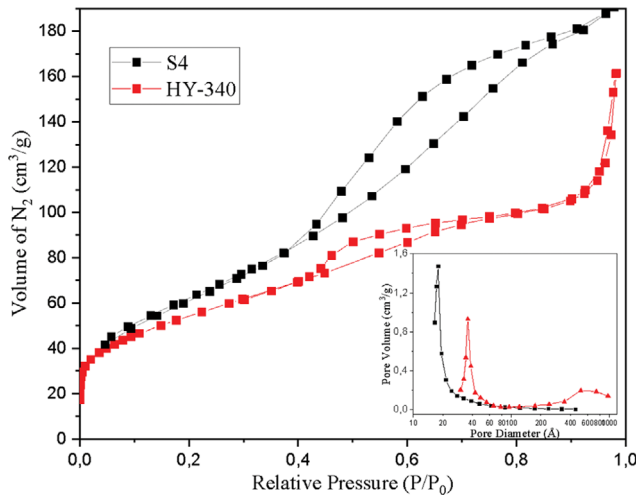


**Fig. 2. $N_2$-adsorption-desorption isotherms of S4 and HY-340 catalysts and pore size distribution curves (inset) generated by the BJH method from the $N_2$ desorption isotherms.**

**Table 1. Acid sites amount determined by titration method and concentration of Brønsted and Lewis acid sites determined by FTIR of adsorbed pyridine for the samples**

| Sample | Bronsted acid sites (mmol/g) | Lewis acid sites (mmol/g) | Acid sites ($H^+$/g) |
|---|---|---|---|
| S4 | 0.211 | 0.283 | $173.41\times10^{19}$ |
| HY-340 | 0.129 | - | $163.84\times10^{19}$ |

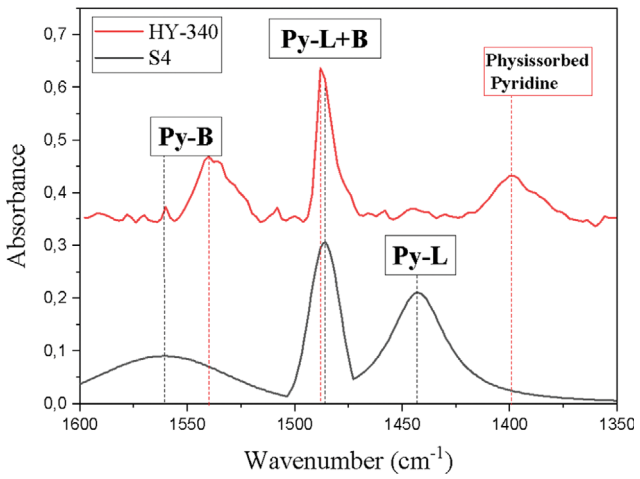


**Fig. 3. FT-IR spectra of pyridine adsorbed on S4 and HY-340 samples.**

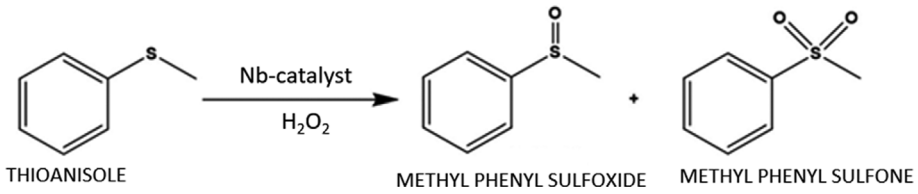


**Scheme 1. Illustrative representation of the thioanisole oxidation.**

teristic of the vibrational mode of protonated and coordinate pyridine (Py-L+B) and at 1,559 $cm^{-1}$, characteristic of the Brønsted acid site (Py-B). For the HY-340 commercial sample, only the bands at 1,489 $cm^{-1}$ (Py-L+B) and at 1,540 $cm^{-1}$ (Py-B) were found. The synthesized S4 sample has higher density of acid sites (Brønsted+Lewis) than the HY-340 commercial sample (Table 1). Brønsted acid sites are commonly associated with hydroxyl groups that act as proton donors. Lewis acid sites refer to the coordinate and unsaturated surface cations of $Nb^{5+}$ [41]. The surface acidity of the samples was also investigated by liquid-phase acid-base titration (Table 1). The HY-340 sample had $163.84\times10^{19}$ $H^+$ sites/g, which was less than that presented by S4 sample, $173.41\times10^{19}$ $H^+$ sites/g. This indicates that the synthesized S4 sample possess a higher acidity on its surface and, therefore, in this sample, there is a higher hydroxylation level on the surface [42].

**2. Catalytic Activity**

After the synthesis and characterization of the catalysts, we were interested in evaluating how the catalytic performance was dependent upon their structure. The catalysts were evaluated in the oxidation of thioanisole. Through this process, two products were obtained, methyl phenyl sulfoxide and methyl phenyl sulfone, as can be seen in Scheme 1. Previously, control experiments were conducted without catalyst under the same conditions of the catalytic tests. In these situations, it was not possible to observe significant thioanisole conversion.

The effect of the mass of the solid on the catalytic behavior was investigated, Fig. 4. In both cases (S4 and HY-340 samples), an increase in the catalyst mass led to an increase in the activity and a rise in the selectivity toward methyl phenyl sulfone. The S4 catalyst showed the highest activity and selectivity toward methyl phenyl sulfone, in each reaction condition. Higher conversion was achieved with 10 mg of catalyst. Therefore, this catalyst amount was used in the subsequent reactions. Fig. 5 shows thioanisole conversion and product selectivity values as a function of time. The synthesized S4 catalyst was the most active, promoting higher thioanisole conversion, around 91.6% in 2 hours of reaction. The difference between the specific surface areas may have contributed to the differences in the activities presented by the catalysts. The specific surface area of a catalyst plays a pivotal role, as an increase in the catalytic surface reduces the amount of catalyst required for a process [42]. The S4 catalyst presented greater specific surface area and pore volume than the commercial sample. This factor can be correlated with the catalytic sites more available to adsorb the oxidant and the large molecule of the reagent. Additionally, as it can be seen in the diffractograms, S4 catalyst presents lower crystallinity than HY-340. According to Ziolek and co-workers [10], in their experiments with niobium and tantalum oxides, catalysts with lower crystallinity may have higher availability of hydrogen peroxide activating surface groups. This characteristic is more useful in generating reactive oxygen species, which contributes directly toward oxidation pro-

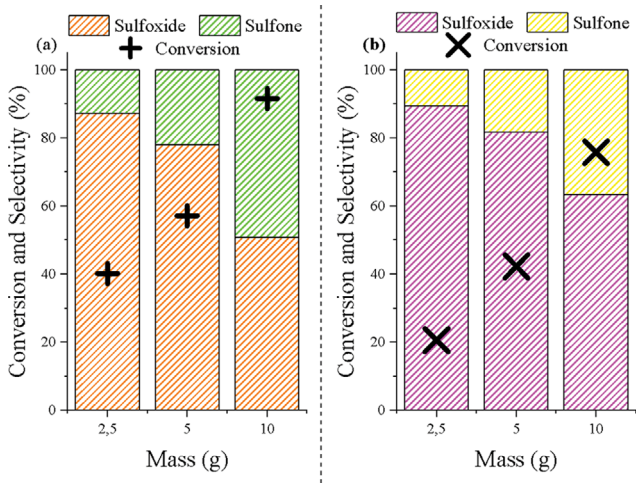


**Fig. 4. (a) Conversion and selectivity of the reaction of thioanisole oxidation using S4 and (b) Conversion and selectivity of the reaction of thioanisole oxidation using HY-340. Conditions: $H_2O_2$ volume=0.1 mL, T=25 °C, t=2 h and solvent=acetonitrile.**

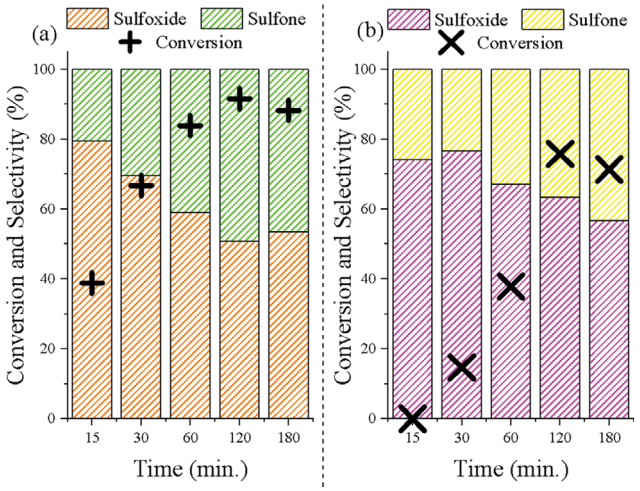


**Fig. 5. (a) Kinetic and selectivity of the reaction of thioanisole oxidation using S4 and (b) Kinetic and selectivity of the reaction of thioanisole oxidation using HY-340. Conditions: $H_2O_2$ volume=0.1 mL, solvent=acetonitrile, T=25 °C and catalyst mass=10 mg.**

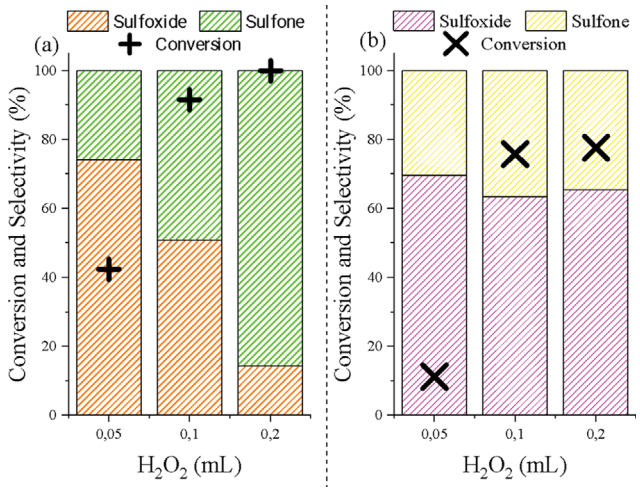


**Fig. 6. (a) Conversion and selectivity of the reaction of thioanisole oxidation using S4 and. (b) Conversion and selectivity of the reaction of thioanisole oxidation using HY-340 in relation to the volume of peroxide. Conditions: solvent=acetonitrile, T= 25 °C, t=2 h and catalyst mass=10 mg.**

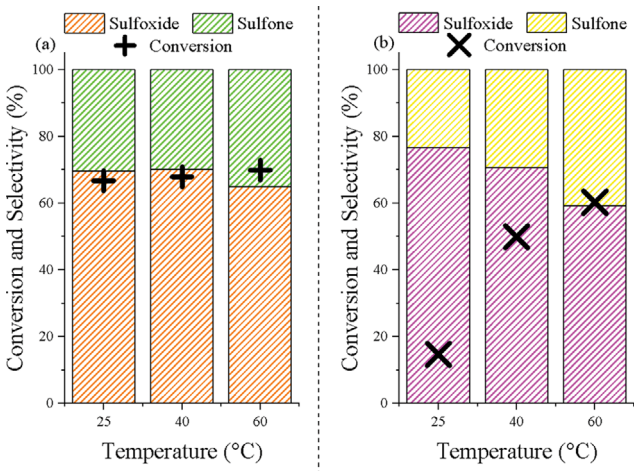


**Fig. 7. (a) Kinetic and selectivity of the reaction of thioanisole oxidation using S4 and (b) Kinetic and selectivity of the reaction of thioanisole oxidation using HY-340. Conditions: $H_2O_2$ volume=0.1 mL, catalyst mass=10 mg, t=30 min and solvent= acetonitrile.**

cesses. Correlating these two characterization results, it can be inferred that the S4 material has a greater number of defects available, deduced by the lower crystallinity, from the X-ray diffractograms, and higher specific surface area, revealed by the BET method. These defects can promote more efficient interaction with the reagent molecules and the oxidant, generating greater amount of reactive oxygen species [42]. In relation to the selectivity profile for these catalysts, the behaviors are similar during all the reaction time, that is, an increase in methyl phenyl sulfone formation with time, but S4 catalyst presenting further advantage to formation of the advanced oxidation reaction product. The influence of oxidant volume present in the reaction medium on the catalytic performances was evaluated. Fig. 6 shows the thioanisole conversions and selectivity for two hours of reaction. Both catalysts show a decrease in thioanisole conversion values when half of the $H_2O_2$ volume (0.05 mL) was employed, being about 42.3% for S4. When the maximum volume used (0.2 mL), both catalysts show an increase in the conversion, reaching 100% over S4. It was noticed that there is a propensity to improve the conversion of thioanisole with increasing $H_2O_2$ amounts. This is due to the increase in active oxidizing species available for catalysis. It is possible to see from the results that, for S4 catalyst, a greater selectivity toward methyl phenyl sulfoxide is achieved when using a smaller amount of $H_2O_2$, around 74.2%, but it is totally the opposite case when using a larger volume of oxidant, 85.7% of selectivity toward methyl phenyl sulfone. This is not possible to visualize for the HY-340 catalyst, as the variation in selectivity in relation to the $H_2O_2$ volume is very small. The catalytic performance was also investigated as a function of the reaction temperature (Fig. 7). The thioanisole conversion and selectivity toward methyl phenyl sulfone increased with the temperature over HY-340 catalyst, achieving the highest conversion at 60 °C. On the other hand, for the S4 catalyst, the increase in temperature had no impact on catalytic behavior. Activity and selectivity practically remained unchanged. Probably, the interaction of $H_2O_2$ with the surface of this catalyst

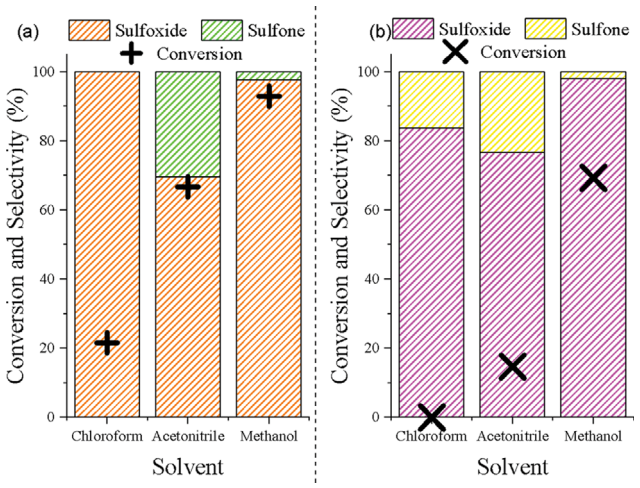


**Fig. 8. (a) Conversion and selectivity of the reaction of thioanisole oxidation using S4 and (b) Conversion and selectivity of the reaction of thioanisole oxidation using HY-340. Conditions: $H_2O_2$ volume=0.1 mL, T=25 °C, t=30 min and catalyst mass= 10 mg.**

was quite effective even at lower temperatures due to the amount of acidic sites (Brønsted and Lewis) on its surface. Finally, the catalytic oxidation was investigated in different solvents (Fig. 8). A relationship with their polarity was evidenced. The thioanisole conversion increased with the polarity of the solvents. Previous results indicated that the thioanisole conversion increases with solvent polarity and that protic solvents can favor high conversion [43].

To check the surfaces, S4 and HY-340 can act as a catalyst for chemical reactions with $H_2O_2$ and thioanisole; single point calculations for developing the potential energy curves (PEC) were carried out between the surface catalyst and $H_2O_2$ as well as thioanisole. Structures of the studied scenarios are reported in Fig. 9. Fig. 10 and Fig. 11 shows the potential energy curve for the compounds. Ana-

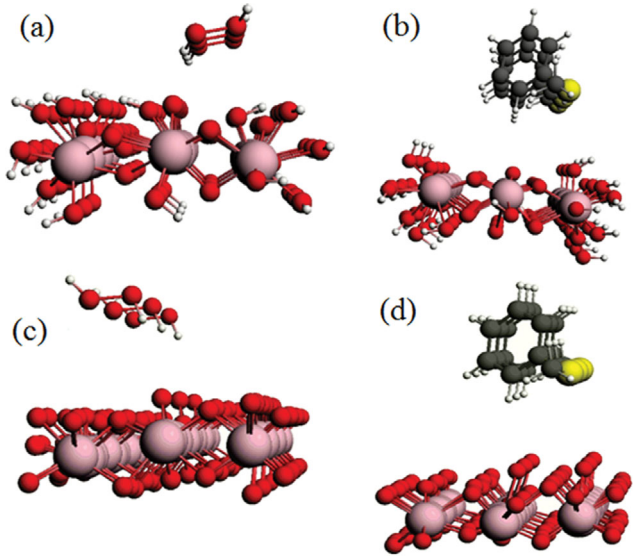


**Fig. 9. Structure (a) S4 with $H_2O_2$ and (b) S4 with thioanisole; structure (c) HY-340 with $H_2O_2$ and (d) HY-340 with thioanisole.**

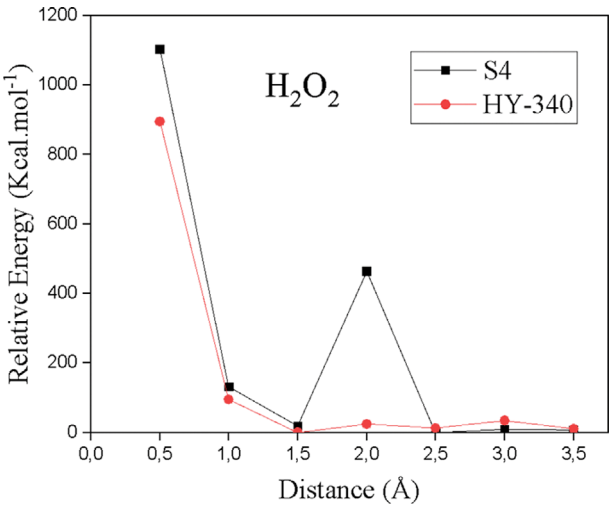


**Fig. 10. Potential energy curve obtained for HY-340 and S4 with $H_2O_2$.**

lyzing the results for the $H_2O_2$ molecule (Fig. 10(a)), for the HY-340 catalyst, it is observed that adsorption takes place between the surfaces; when both structures are very close, the energy of the system increases because of the repulsion between them. However, when they are moved away, the system finds a minimum of energy and remains almost unchanged. For the S4 catalyst, the adsorption process between surfaces occurs; however, at a distance of 2 Å, a transition state is formed. This transition state occurs because of the strong interaction between the OH group of the peroxide molecule and the oxygen atom of the catalyst. In this line, it is important to note that a chemical reaction occurs in the $H_2O_2$ molecule [44]. For thioanisole (Fig. 10(b)), an adsorption with both surfaces, S4 and HY-340, can occur. For S4, when the molecules are apart, position at 3 Å and 3.5 Å. It has little attraction between the molecules; thus, the repulsion force is higher and the energy of the system

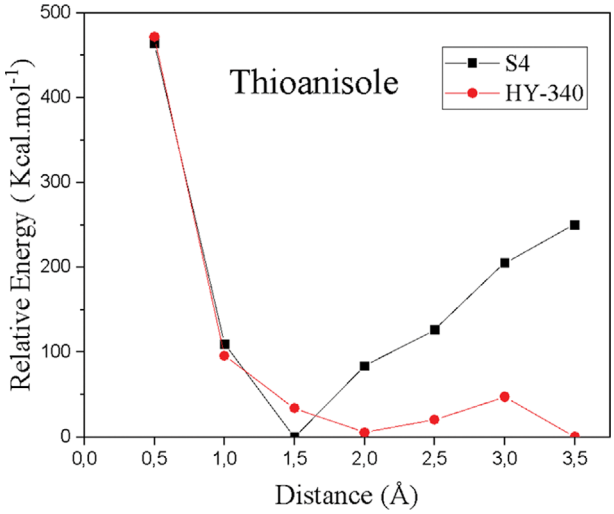


**Fig. 11. Potential energy curve obtained for HY-340 and S4 with thioanisole.**

goes up again. On the HY-340 surface, there is a repulsion between the surfaces at a distance of 3 Å; after that distance, it is observed that the energy falls again at a distance of 3.5 Å. In general, S4 catalyst interacts better with $H_2O_2$ and thioanisole, compared to HY-340 catalyst. This is because on S4 catalyst surface there are more OH groups and they interact more strongly, by hydrogen bonds, with both $H_2O_2$ and thioanisole molecules. This better interaction of S4 catalyst with both oxidant and thioether may help, together with the characterization results, to understand the superior performance to the conversion of the substrate. In fact, it is known that the surfaces of both catalysts HY-340 ($Nb_2O_5{\cdot}nH_2O$) and S4 ($NbO_2OH$) are covered by hydroxyl groups, which makes them capable to form surface peroxo, hydroperoxo, and superoxo species in contact with the oxidant [9,41]. In addition to the FTIR-pyridine adsorption experiments, titration results showed that the amount of acid sites found for the S4 sample was higher than that for HY-340 and, given that, it can be inferred that the former has a higher hydroxylation level on its surface [42]. Considering that for the formation of the reactive peroxo species, from the adsorption of $H_2O_2$ on the Nb-catalyst surface, there is substitution of the surface hydroxyl groups, the greater presence of these groups on the S4 surface leads to an increase in the formation of peroxo species, generating active species that are better suited to catalyze the thioanisole oxidation reaction [10,13]. Fig. 12 compares the activity of the S4 catalyst with other materials presented in the literature. It is interesting to note that the performance of the synthesized catalyst in this study is comparable or superior to those previously reported. Despite some differences in the reaction conditions, the S4 solid showed great potential for the thioanisole oxidation, reaching the highest conversion and selectivity for sulfone out of all the materials listed, and obtaining a satisfactory selectivity for sulfoxide. Moreover, it is important to highlight that the catalyst proposed operated efficiently under mild reaction conditions. This modest comparison of the activity with other reported catalysts indicates that the S4 catalyst can be considered as a good candidate for the thioanisole oxidation reaction [45-49].

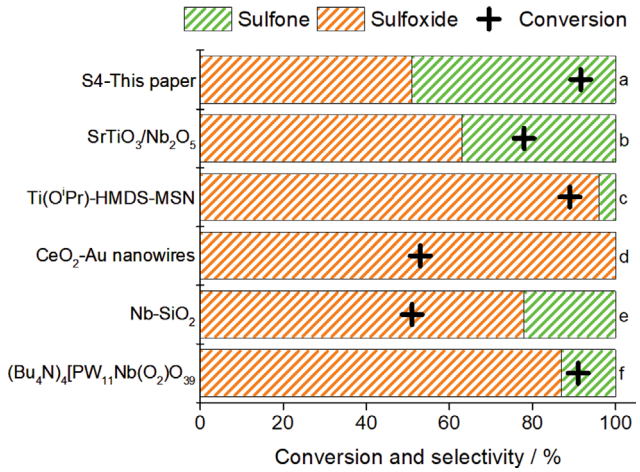


**Fig. 12. Comparative the activity of the S4 catalyst with other materials presented in the literature.**

## CONCLUSIONS

The potential of a new, synthesized niobium oxyhydroxide catalyst (S4) was evaluated in the thioanisole oxidation. Its performance was compared with a commercial niobium oxide catalyst (HY-340). The main surface characteristics of both materials were investigated, such as specific surface area, crystallinity and acidic sites. The S4 synthesized catalyst presented the highest specific surface area, lowest crystallinity and greater surface acidity, which directly reflect in the thioanisole conversion reaching 100%, with 0.2 mL of $H_2O_2$, in a short time and at room temperature. Additionally, this solid showed more efficiency for the methyl phenyl sulfone formation, almost 90%, probably due to the greater ability in the generation of oxygen reactive species. According to theoretical investigations, this is because of the better interaction of $H_2O_2$ and thioanisole molecules with the surface of this catalyst, due to its higher degree of surface hydroxylation, leading S4 to the best performance in the thioanisole oxidation process.

## ACKNOWLEDGEMENTS

This work was supported by the Conselho Nacional de Desenvolvimento Científico e Tecnológico - CNPQ, Coordenação de Aperfeiçoamento de Pessoal de Nível Superior - CAPES and Fundação de Amparo à Pesquisa do Estado de Minas Gerais - FAPEMIG.

## REFERENCES

1. C. Bruziquesi, J. Balena, M. Pereira, A. Silva and L. Oliveira, *Quim Nova*, **42**(10), 1184 (2019).
2. A. R. Alves and A. dos Reis Coutinho, *Mater. Res.*, **18**(1), 106 (2015).
3. K. Tanabe and S. Okazaki, *Appl. Catal. A-Gen.*, **133**(2), 191 (1995).
4. M. Ziolek and I. Sobczak, *Catal. Today*, **285**, 211 (2017).
5. I. Nowak and M. Ziolek, *Chem. Rev.*, **99**(12), 3603 (1999).
6. K. Tanabe, *Catal. Today*, **78**(1), 65 (2003).
7. M. Ziolek, *Catal. Today*, **78**(1), 47 (2003).
8. D. C. Batalha and M. J. da Silva, *Energies*, **14**(17), 5506 (2021).
9. K. Skrodczky, M. M. Antunes, X. Han, S. Santangelo, G. Scholz, A. A. Valente, N. Pinna and P. A. Russo, *Commun. Chem.*, **2**(129), 1 (2019).
10. M. Ziolek, I. Sobczak, P. Decyk, K. Sobańska, P. Pietrzyk and Z. Sojka, *Appl. Catal. B-Environ.*, **164**, 288 (2015).
11. M. Ziolek, I. Sobczak, P. Decyk and L. Wolski, *Catal. Commun.*, **37**, 85 (2013).
12. M. B. Pinto, A. L. Soares, M. C. Quintão, H. A. Duarte and H. A. de Abreu, *J. Phys. Chem. C*, **122**(12), 6618 (2018).
13. C. M. Silva, P. L. Silva and J. R. Pliego, *J. Phys. Chem. C*, **124**(17), 9369 (2020).
14. A. C. Silva, R. M. Cepera, M. C. Pereira, D. Q. Lima, J. D. Fabris and L. C. A. Oliveira, *Appl. Catal. B-Environ.*, **107**(3-4), 237 (2011).
15. T. Punniyamurthy, S. Velusamy and J. Iqbal, *Chem. Rev.*, **105**(6), 2329 (2005).
16. J. Přech, R. E. Morris and J. Čejka, *Catal. Sci. Technol.*, **6**(8), 2775 (2016).
17. S. Doherty, J. G. Knight, M. A. Carroll, J. R. Ellison, S. J. Hobson, S. Stevens, C. Hardacre and P. Goodrich, *Green Chem.*, **17**(3), 1559 (2015).
18. P. Cruz, M. Fajardo, I. del Hierro and Y. Pérez, *Catal. Sci. Technol.*, **9**, 620 (2019).
19. B. K. Kundu, M. Das, R. Ganguly, P. A. Bhobe and S. Mukhopadhyay, *J. Catal.*, **389**, 305 (2020).
    a) Ammar T. Khadim, Talib M. Albayati and Noori M. C. Saady, *Microp. Mesop. Mat.*, **341**, 112020 (2022).
    b) Ammar T. Khadim, Talib M. Albayati and Noori M. Cata Saady, *Environ. Nanotechnol., Monitoring Manage.*, **17**, 100635 (2022).
20. R. Fazaeli, H. Aliyan, M. A. Ahmadi and S. Hashemian, *Catal. Commun.*, **29**, 48 (2012).
21. A. Bayat, M. Shakourian-Fard and M. M. Hashemi, *Catal. Commun.*, **52**, 16 (2014).
22. F. Rajabi, S. Naserian, A. Primo and R. Luque, *Adv. Synth. Catal.*, **353**, 2060 (2011).
23. Q. Wang, W. Ma, O. Tong, G. Du, J. Wang, M. Zhang, H. Jiang, H. Yang, Y. Liu and M. Cheng, *Sci. Rep.*, **7209**, 7 (2017).
24. L. Fang, Q. Xu, Y. Qi, X. Wu, Y. Fu, Q. Xiao, F. Zhang and W. Zhu, *Mol. Catal.*, **486**, 110863 (2020).
25. K. S. Ravikumar, J. P. Bégué and D. Bonnet-Delpon, *Tetrahedron. Lett.*, **39**, 3141 (1998).
26. V. Ayala, A. Corma, M. Iglesias and F. Sánchez, *J. Mol. Catal. A Chem.*, **221**, 201 (2004).
27. B. Karimi, M. Ghoreishi-Nezhad and J. H. Clark, *Org. Lett.*, **7**, 625 (2005).
28. K. Sato, M. Hyodo, M. Aoki, X. Q. Zheng and R. Noyori, *Tetrahedron*, **57**, 2469 (2001).
29. J. Zhang, T. Jiang, Y. Mai, X. Wang, J. Chen and B. Liao, *Catal. Commun.*, **127**, 10 (2019).
30. W. Zhao, C. Yang, Z. Cheng and Z. Zhang, *Green Chem.*, **18**, 995 (2016).
31. C. L. Marchena, C. Saux, R. Dinamarca, G. Pecchi and L. Pierella, *RSC Adv.*, **6**, 102015 (2016).
32. A. Feliczak-Guzik, A. Wawrzyńczak and I. Nowak, *Micropor. Mesopor. Mat.*, **202**, 80 (2015).
33. J. B. Gabriel, V. Oliveira, T. E. Souza, I. Padula, L. C. A. Oliveira, L. V. A. Gurgel, B. E Baeta and A. C. Silva, *ACS Omega*, **5**, 21392

(2020).
34. M. J. Frisch, G. W. Trucks, H. B. Schlegel, G. E. Scuseria, M. A. Robb, J. R. Cheeseman and J. A. Pople, "Handbook of Gaussian" Gaussian, Inc (2004).
35. T. E. Souza, I. D. Padula, M. M. Teodoro, P. Chagas, J. M. Resende, P. P. Souza and L. C. Oliveira, *Catal. Today*, **254**, 83 (2015).
36. T. E. Souza, M. F. Portilho, P. M. T. G. Souza, P. P. Souza and L. C. A. Oliveira, *ChemCatChem*, **6**, 2961 (2014).
37. R. Guidelli, R. G. Compton, J. M. Feliu, E. Gileadi, J. Lipkowski, W. Schmickler and S. Trasatti, *Pure Appl. Chem*., **87**, 1051 (2015).
38. E. N. Alvar, M. Rezaei and H. N. Alvar, *Powder Technol*., **198**, 275 (2010).
39. Z. Zhao, L. Zhang, H. Dai, Y. Du, X. Meng, R. Zhang, Y. Liu and J. Deng, *Micropor. Mesopor. Mater.*, **138**, 191 (2011).
40. H. Li, G. Wang, F. Zhang, Y. Cai, Y. Wang and I. Djerdj, *RSC Adv.*, **2**, 12413 (2012).
41. S. M. A. Hakim Siddiki, N. Rashed, A. Ali, T. Toyao, P. Hirunsit, M. Ehara and K. Shimizu, *ChemCatChem*, **11**, 383 (2019).
42. D. C. Batalha, N. H. Marins, R. M. Silva, N. L. V. Carreno, H. V. Fajardo and M. J. da Silva, *Mol. Catal*., **489**, 110941 (2020).
43. Z. T. Alismaeel, T. M. Al-Jadir, T. M. Albayati, A. S. Abbas and A. M. Doyle, *Adv. Powder Technol*., **33** (2022).
44. T. F. Rosado, M. P. Teixeira, L. C. Moraes, L. A. da Silva, A. V. Pontes-Silva, J. G. Taylor, I. C. de Freitas, D. C. de Oliveira, J. Gardener, G. Solórzano, T. V. Alves, M. F. Venancio, M. I. P. da Silva, E. Brocchi, H. V. Fajardo and A. G. M. da Silva, *Appl. Catal., A*, **613**, 118010 (2021).
45. A. M. Mesquita, I. R. Guimaraes, G. M. M. de Castro, M. A. Goncalves, T. C. Ramalho and M. C. Guerreiro, *Appl. Catal., B*, **192**, 286 (2016).
46. F. C. Riemke, C. L. Ucker, N. L. V. Carreno, S. S. Cava, M. P. Teixeira, H. V. Fajardo, J. G. Taylor, M. J. Silva, D. C. Batalha and C. W. Raubach, *Mat. Chem. Phys*., **278**, 125591 (2022).
47. P. Cruz, M. Fajardo, I. del Hierro and Y. Perez, *Catal. Sci. Technol*., **9**, 620 (2018).
48. N. E. Thornburg and J. M. Notestein, *ChemCatChem*, **9**, 3714 (2017).
49. O. V. Zalomaeva, N. V. Maksimchuk, G. M. Maksimov and O. A. Kholdeeva, *Eur. J. Inorg. Chem*., **2019**, 410 (2019).